Progress in the fabrication of optical fibers by the sol-gel-based granulated silica method

S. Pilz[a], H. Najafi[a], A. El Sayed[a,b], J. Boas[a], D. Kummer[a], J. Scheuner[b], D. Etissa[b], M. Ryser[b], P. Raisin[b], S. Berger[c], V. Romano[a,b]

[a] Bern University of Applied Sciences, ALPS, Pestalozzistrasse 20, CH-3400 Burgdorf, Switzerland
[b] Institute of Applied Physics, University of Bern, Sidlerstrasse 5, CH-3012 Bern, Switzerland
[c] ReseaChem GmbH, Pestalozzistrasse 16, CH-3400 Burgdorf, Switzerland

ABSTRACT

Novel special optical fibers nowadays can take advantage of several new preform production techniques. During the last years we have devoted our attention to the granulated silica method. It is one of the variants of the powder-in-tube technique and potentially offers a high degree of freedom regarding the usable dopants, the maximum possible dopant concentration, the homogeneity of the dopants, the geometry and minimal refractive index contrast. We developed and refined an approach for the production of doped granulated silica material based on the sol-gel process.

Here, we present material analysis results of an ytterbium (Yb) doped, aluminum (Al) and phosphorous (P) co-doped glass on the basis of our sol-gel glass based granulated silica method as well as first measurements of two LMA fibers obtained from this material. For the material analysis we used advanced analysis techniques, such as HAADF-STEM and STEM-EDX spectroscopy to determine the composition of the material and the distribution of the dopants and the co-dopants. The chemical mapping of the STEM-EDX shows an extremely homogeneous distribution of the dopants and co-dopants in nano-scale. Based on self-made LMA fibers, we measured the refractive index contrast of the sol-gel-based granulated silica derived core compared to the pure silica cladding. In addition we quantified optical characteristics such as the emission and absorption spectrum. The measured upper state lifetime of the optical active dopant ytterbium was 0.99ms, which in turn confirms the homogeneous distribution of the Yb atoms. The propagation losses were determined to be 0.2dB/m at 633nm and 0.02414dB/m at1550nm.

Keywords: Granulated silica, sol-gel, optical fibers, Yb doped fiber, large mode area fibers, fiber preform

1. INTRODUCTION

Special optical fibers such as e.g. fibers with a non-cylindrical shape (e.g. microstructured fibers such as leakage channel fibers (LCFs)), high doping concentration of the active element and a large core (large mode area (LMA) fibers) have been intensively investigated over the last years [1-9]. With our sol-gel-based granulated silica method approach we merge the benefits of the granulate based on sol-gel with the advantages of the powder-in-tube technique. The benefits of the sol-gel-based granulated silica method are manifold. First, the sol-gel process offers a high degree of freedom and simplicity concerning the optically active applicable dopants (rare earth) and passive co-dopants (e.g. phosphorous, aluminum, graphene). With this method we can incorporate dopants that otherwise are difficult to be added in a controlled way. This freedom in controlling the co-dopants and their concentration on the other hand enables the full control respectively to tailor the refractive index. Secondly, a high dopant concentration up to several at.% can be reached [10]. Next, the glass derived from the sol-gel-based granulated silica features a high homogeneity (in nano-scale), since every grain of the granulate is homogenously doped. By virtue of the powder-in-tube technique we also gain versatility in producing any kind of fiber structure since no symmetry is required. Last but not least, the powder-in-tube technique allows us a rapid production of preforms from in-stock sol-gel-based granulated silica. Thus, by using our granulated silica method based on the sol-gel process, we can complement the conventional preform production techniques such as e.g. the modified chemical vapor deposition (MCVD) method. MCVD preforms are best suited for fiber shapes with a cylindrical symmetry and furthermore, due to the complexity of the MCVD process and the time

Micro-Structured and Specialty Optical Fibres IV, edited by Kyriacos Kalli, Alexis Mendez, Proc. of SPIE Vol. 9886, 988614 · © 2016 SPIE
CCC code: 0277-786X/16/$18 · doi: 10.1117/12.2227569

consuming layer-by-layer deposition, the dopant concentration is limited and the core size is restricted by reason of homogeneity.

Our sol-gel-based granulated silica method allows us to produce optically passive as well as active sol-gel-based material, that features a high rare earth dopant (e.g. ytterbium) content with the possibility to tailor the refractive index by means of co-dopant concentration (e.g. aluminum and phosphorous, where the phosphorous can compensate the refractive index change arising from the aluminum [11]) and therefore to control the refractive index contrast. By using this material for the powder in-tube-preform production technique we have full freedom to fabricate fibers with any geometry including microstructured fibers such as LCF (Leakage Channel Fibers) and LMA fibers (Large Mode Area) with no limitations to the core diameter due to inhomogeneity. Here we present the progress achieved in the fabrication of optical fibers by the sol-gel-based granulated silica method.

2. METHOD

We have developed and refined an approach for the production of granulated silica material based on the sol-gel process. First, we give a brief overview of the basic principle of our approach, which is shown in Figure 1, before we will explain our approach in detail.

The sol-gel process starts with mixing resp. dissolving alkoxide precursors in the liquid phase and at room temperature (which is one big advantage of this method), see Figure 1. This process has the benefit to reach high dopant concentrations with a high homogeneity with considerable less effort than traditional glass production methods and enables a greater freedom in adaptable dopants. Furthermore it has been reported that silica powder based on the sol-gel method shows lower impurities compared with natural quartz powder which is commonly used for pure silica glass [12]. Therefore the sol-gel method is perfectly suited to manufacture (e.g. rare earth) doped material for the fiber production. By the addition of water and by moderate heating and stirring the mixture undergoes hydrolysis, condensation and gelatinization and finally results in a gel. This gel is then dried into a powder where every gain is homogenously doped. Subsequently, the dried powder is then sintered. The resulting sintered powder block is then manually pestled and furthermore we selected grain sizes between 150um and 1mm by sieving them out. From now on, the sintered and size selected powder is referred as granulate. This granulate can be used in principle directly for the powder-in-tube technique. However, if we use this granulate directly in the preform, the evacuation becomes an issue which in turn leads to high propagation losses and scattering centers. Based on our previous studies, we found, that an intermediate vitrification step of the granulate (e.g. “small zone vitrification technique” [13] before fiber drawing of (at least) the guiding region of the fiber will improve the propagation resp. the scattering losses of the resulting fiber.

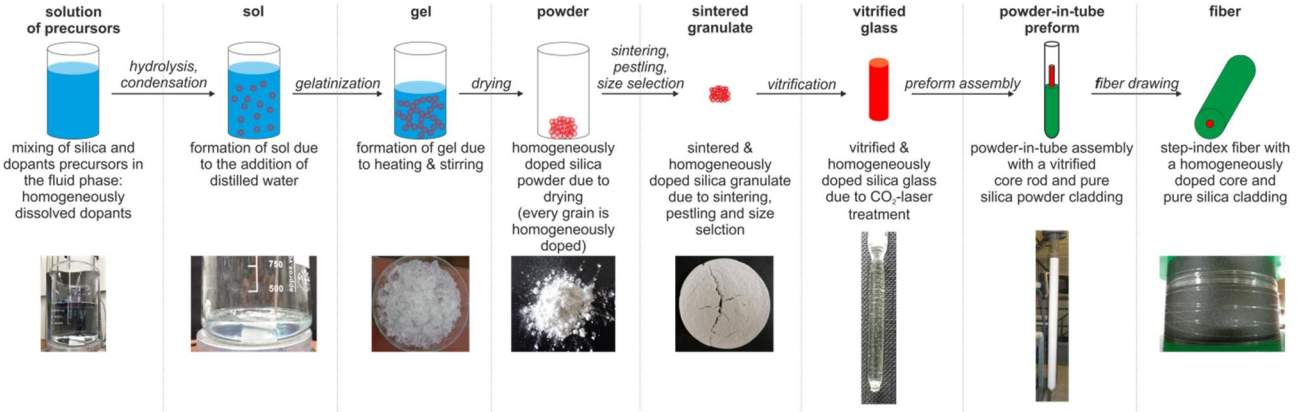

Figure 1: Basic principle of our developed and refined sol-gel process approach.

It should be mentioned that over the last years we not only investigated the granulated silica method based on sol-gel process but also the granulated silica method based on direct mixing of oxide powders [14,15]. The main drawback of the oxides based method compared to the sol-gel approach is a homogeneity issue. Since only mixing oxides together, will not result in a homogeneously doped glass, an complex and multi-step iterative CO_2-laser melting and milling treatment is needed [14,15]. However, as mentioned before, the sol-gel-based approach solves this issue, since the material is already homogenously doped in nano-scale without any (iterative) CO_2-laser treatment. Figure 2 shows the

improvement regarding the homogeneity of the sol-gel approach based on high angle annular dark-field scanning transmission electron microscopy (HAADF-STEM) images.

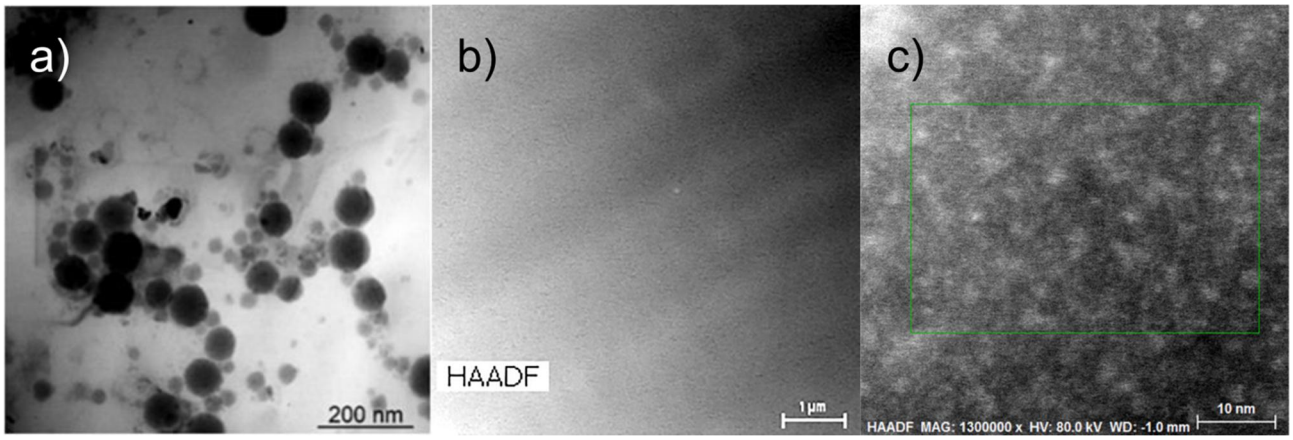

Figure 2: HAADF STEM images of a) doped material derived from the direct oxides mixing method shows clustering of the dopants; b) & c) doped material derived from the sol-gel process, shows homogeneous distribution and no clustering.

Yb,Al, P doped granulated silica based on the sol gel process

Since we are interested in fabricating a fiber with emission within the near infrared region of 1000-1100nm, the rare earth (RE) element ytterbium (Yb) is our active element of choice. Furthermore we used two optically passive co-dopants: aluminum (Al) and phosphorous (P). Aluminum is used, since it is known on the one hand to increase the solubility of RE elements (in our case Yb) [16] and on the other hand to prevent clustering of the RE element. While phosphorous (P) is known to reduce the photo darkening. Both co-dopants by their own would individually increase the refractive index, but in combination one can use the phosphorous to compensate the refractive index change arising from the aluminum [3]. We used the liquid tetraethyl orthosilicate (TEOS: $Si(OC_2H_5)_4$) as silica precursor for our sol-gel process.

We start our sol-gel process with dopant and co-dopant precursors in powder form. In a first step, the (optically active) dopant precursor ytterbium(III) nitrate pentahydrate ($Yb(NO_3)_3 \cdot 5H_2O$) and the (optically passive) co-dopant precursors aluminum nitrate nonahydrate ($Al(NO_3)_3 \cdot 9H_2O$) and phosphorus pentoxide (P_2O_5) are solved altogether in ethanol, while TEOS is separately solved in ethanol. Next, both before mentioned solutions are mixed together and stirred at room temperature. Then, we used and added hydrochloric acid (HCl) as a catalyst and to keep the pH lower than 6. By the addition of de-ionized water and additional moderate heating in the region of 70-80°C, the mixed solution undergoes hydrolysis, condensation and gelatinization with the result of the formation of a gel after few hours. This gel is then dried into a powder where already every gain is homogenously doped. After the drying step, the dried powder undergoes a sintering routine. The powder is slowly heated up by a rate of 2 C°/min till 1550°C is reached. Then the temperature is kept at 1550°C for several hours, before it is cooled down to room temperature with the same rate of 2 C°/min. During the sintering process, residual impurities are eliminated and the powder is densified. Furthermore a block of powder was formed, as can see Figure 1. This block of powder is then manually pestled and sieved to a grain size of 150μm-1mm, and is from now on referred as granulate. The grain size itself and the size distribution of the granulate is an important parameter for the evacuation during the vitrification or direct fiber drawing process.

Preliminary studies showed that directly using this granulate in a preform tube, where the glass transition take place during the drawing process will result in a fiber with high propagation losses and scattering centers [14,15]. By an additional vitrification step, where especially the fiber regions that guide the light (always the core, for double-clad fiber the cladding as well) are vitrified before drawing, the propagation losses and the scattering centers can be reduced [14,15]. By using the "small zone vitrification technique" which is based on a CO_2-laser treatment [13], we can vitrify tubes up to 5mm that are filled with granulate into so called vitrified core rods, see Figure 3a). Based on these vitrified core rods we can use two different preform assembly variations. The vitrified core rod can now be either centered in a larger preform tube, where the remaining space is then filled up with pure silica granulate (Figure 3b)) or in a larger preform tube with thick pure silica walls, where the diameter if the tube cavity matches the diameter of the vitrified core rod (Figure 3c)). The first variant was used together with a high index coating to draw a single-clad fiber whereas the second variant was used together with a low index coating to draw a double-clad fiber.

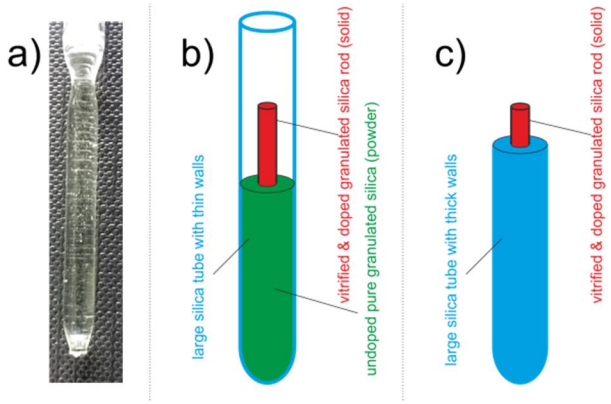

Figure 3: a) Vitrified core rod manufactured by the "small zone vitrification technique". b) The vitrified core rod is centered in a larger preform tube and the remaining space is filled up with pure silica granulate. c) The vitrified core rod is placed in a larger preform tube with thick pure silica walls and matching diameter of the vitrified core rod and the tube cavity.

3. RESULTS AND DISCUSSION

Composition

At the beginning of the sol-gel process we used the following atomic/molar percentage ratio of the precursors:

TEOS / at.%	$Yb(NO_3)_3 \cdot 5H_2O$ / at.%	$Al(NO_3)_3 \cdot 9H_2O$ / at.%	P_2O_5 / at.%
94.72	0.3	3.12	1.86

After the fiber drawing we analyzed and determined the composition of the fiber core, which is derived from our above mentioned sol-gel precursor composition, by using energy-dispersive x-ray spectroscopy of a scanning electron microscope (SEM-EDX). The EDX spectrum is shown in Figure 4 and the corresponding mass percentages are as follows:

Si / m.%	O / m.%	Yb / m.%	Al / m.%	P / m.%
42.40	54.04	1.39	1.26	0.91

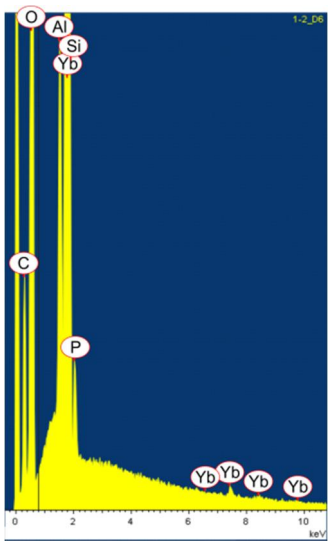

Figure 4: EDX spectrum from doped fiber core derived from the sol-gel process.

Then we calculated the atomic percentages by neglecting the oxygen (O), since we are interested in the ratio of the dopants Yb, Al and P to the Si host (and not to SiO_2), to be as follows:

Si / at.%	Yb / at.%	Al / at.%	P / at.%
94.72	0.5	2.93	1.84

If we compare the at.% ratio of the precursors and the at.% ratio of the fiber core glass, we see a small difference. This small difference is due to the accuracy of the m.% determination of the EDX and since a small error in the m.% can result in a larger error of at.%. However, we can record that the composition of the precursors is conserved over the whole sol-gel process and fiber drawing.

Homogeneity

To determine the distribution of the all elements (including dopant and co-dopants), respectively the homogeneity of our sol-gel-based material; we used high angle annular dark-field scanning transmission electron microscopy (HAADF-STEM). The chemical mapping of our sol-gel-based fiber core is shown in Figure 5, with the result that no clustering was observed (compare with Figure 2) and an extremely homogeneous distribution of the dopant (Yb) and co-dopants (Al and P) in nano-scale was measured [17].

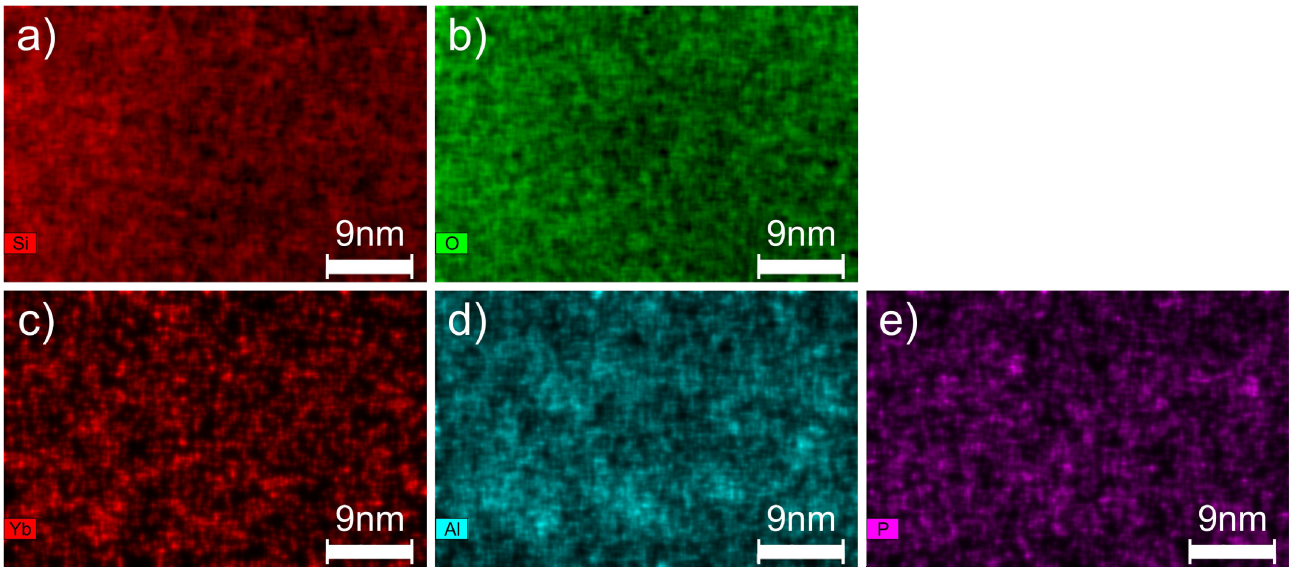

Figure 5: Chemical mapping from STEM shows an extremely homogeneous distribution in nano-scale of a) silicon (Si), b) oxygen (O), c) ytterbium (Yb), d) aluminum (Al) and e) phosphorus (P).

Emission / absorbance spectra

The emission spectrum was recorded by using an ocean optics USB4000 spectrometer and by laterally pumping a vitrified core rod at 915nm. The spectrum is shown in Figure 6a) and it has to be mentioned that we used two long-pass filters at 950nm to block the pump wavelength. One can see in Figure 6a), that the maximal emission peak is at the wavelength of 976nm and agrees with the maximal emission of commercial Yb doped fibers. However, the second broad emission wing at higher wavelength is not centered around 1060nm as for commercial Yb doped fibers, instead it is centered around 1020nm. Consequently the gain, lasing and amplification characteristics cannot be determined in the ordinary wavelength region of 1060-1070nm rather it has to be around 1020nm. The reason for this shift is not yet clarified and investigations are ongoing, but we assume that it is due to the fact that we might have applied different co-dopants then are used for commercial Yb doped fibers.

The absorbance of a 1mm thick vitrified and plane-parallel glass sample was measured by a Perkin Elmer Lambda 750 spectrophotometer and its spectrum is shown in Figure 6b). Our measured absorbance spectrum shows the same features/characteristics and corresponds well with the absorption spectra from commercial fibers. Therefore we can use the standard pump wavelengths of 976nm and 915nm for Yb doped fibers.

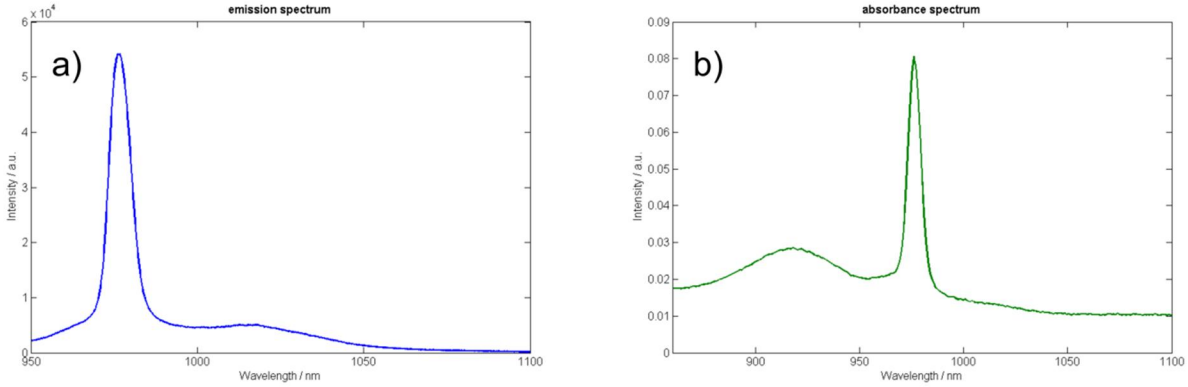

Figure 6: a) Emission spectrum of a vitrified core when pumped at 915nm; b) absorbance spectrum of a 0.5mm thick vitrified and plane-parallel glass sample derived from the sol-gel process.

Lifetime

The average lifetime of the upper laser level of the ytterbium of all our vitrified core rods samples was measured to be τ_{mean}= 0.99ms. According to the literature the lifetime should be around 1ms. This good agreement is a strong indication that no clustering in micro-scale of the dopants occurred and the dopants are homogeneously distributed in the amorphous glass structure.

Fiber geometry

We have used vitrified and doped core rods based on sol-gel with to different preform assembly variation, as mentioned earlier. One of these two variations was used for the production of a single-clad (SC) large mode area (LMA) fiber whereas the other alternative was used for the fabrication of a double-clad (DC) large mode area (LMA) fiber.

First, we used the vitrified core rod (diameter of ≈3.8mm) in a 17x21mm preform tube (closed at one end); where the vitrified core rod was centered and the remaining space was filled with pure silica granulate. This preform was then placed in the drawing furnace and evacuated from the top. Furthermore the drawn fiber was coated with a high refractive index polymer, resulting in a single-clad and LMA fiber. The geometric fiber parameters as well as a microspore image of this SC LMA are illustrated in Figure 7a).

Secondly, we used the vitrified core rod (diameter of ≈3.8mm) in a specially (for that purpose) tailored preform tube with thick walls; where the diameter of the vitrified core rod matches the diameter of the preform tube cavity. This fiber was drawn and a low index polymer was applied, resulting in a double-clad and LMA fiber. The geometric fiber parameters as well as a microspore image of this DC LMA are shown in Figure 7b).

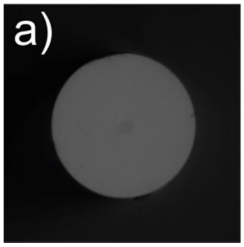

single-clad LMA:

Core diameter	20µm
Cladding diameter	190µm
Coating diameter	400µm
Coating	high index

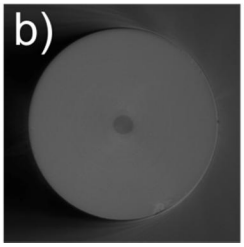

double-clad LMA:

Core diameter	22µm
Cladding diameter	250µm
Coating diameter	400µm
Coating	low index

Figure 7: Microscope images and geometric parameters of a) self-made single-clad LMA fiber; b) self-made double-clad LMA fiber.

Refractive index

The refractive index of both fibers was measured by two diverse methods in order to confirm the results. On the one hand, we used a self-built reflection-based refractive index mapping setup [18], on the basis of a time-consuming scanning technique. And on the other hand, we used a self-built inversed refracted near-field (IRNF) setup [19], which is based on a fast imaging technique.

i) Single-clad LMA

The refractive index profile of the SC LMA fiber based on the reflection-based refractive index mapping method is shown in Figure 8. This Figure shows one line scan as well as the average refractive index of the core and cladding. The

average values are always obtained by scanning and averaging a large area of the core or the cladding, instead of only averaging the line scan. The refractive index difference between the doped fiber core derived from sol-gel and the pure silica fiber cladding derived from pure silica granulate was determined to be $\Delta n = 3.35 \cdot 10^{-3}$. Furthermore, this value was confirmed by the additional IRNF based measurement within the accuracy of the particular method.

ii) Double-clad LMA

The refractive index profile of the DC LMA fiber based on the reflection-based refractive index mapping method is shown in Figure 9, with a resulting refractive index difference between the doped fiber core derived from sol-gel and the pure silica fiber cladding derived from pure silica tube was determined to be $\Delta n = 2.65 \cdot 10^{-3}$. Based on an IRNF based measurement, this value was again confirmed.

The different refractive index contrast of the SC and DC fiber is based on the use of slightly different pure silica material for the cladding. For the SC preform we used pure silica granulate and for the DC preform, a pure silica preform tube with thick walls with a slightly different refractive index was used.

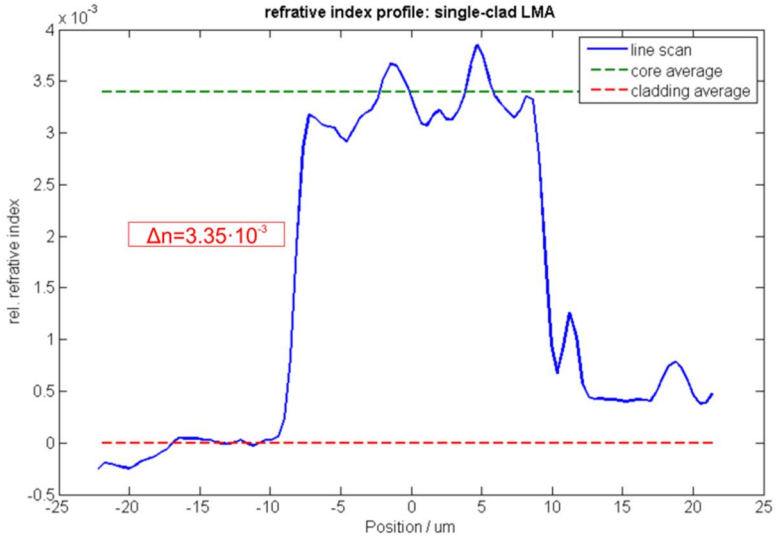

Figure 8: Refractive index profile of the single-clad fiber obtained from the reflection-based refractive index mapping method.

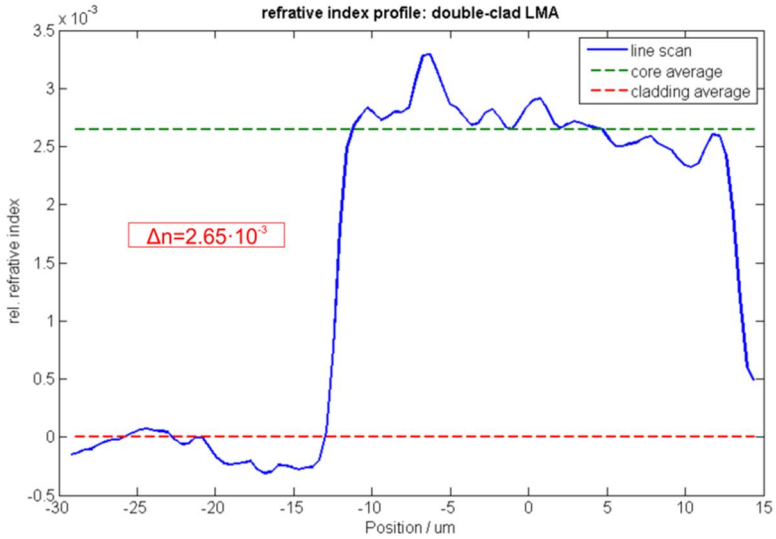

Figure 9: Refractive index profile of the double-clad fiber obtained from the reflection-based refractive index mapping method.

Propagation losses

The propagation losses were determined at two different (not absorbing) wavelengths by two diverse methods. While we used the destructive cutback technique at a wavelength of 633nm, we also used a self-built and non-destructive high-resolution optical time-domain reflectometer (HR-OTDR) setup at 1550nm [20]. Since we are interested in the propagation losses of the fiber core derived from sol-gel, we could only use the single-clad fiber for the propagation loss measurements, because the guiding cladding of the double-clad fiber would influence and falsify the loss measurement. On the basis on the cutback we measured a propagation loss of 0.2dB/m at 633nm, whereas for the HR-OTDR the propagation losses were determined to be 0.02414dB/m at 1550nm. If we do not take the absorption in the near infrared region into account, the estimated propagation losses in this region lie in between the two measured values, and are therefore in principle low enough to use this fiber for fiber laser respectively amplifier applications.

4. CONCLUSION & OUTLOOK

To conclude, we have pointed out the benefits of our sol-gel-based granulate approach for the production of optical fibers. In particular, two large mode area fibers (single-clad and double-clad) with an Yb doped and Al/P co-doped core material derived from our refined sol-gel process have been manufacture. The sol-gel material as well as the fibers have been analyzed and characterized by a diverse suite of advanced analysis technique such as SEM-EDX and HAADF STEM. It was confirmed that the dopant (Yb) and co-dopant (Al, P) concentrations are conserved during our sol-gel and drawing process. Furthermore, the dopants of our sol-gel-based material features no clustering (in nano-scale) and a homogeneous distribution in nano-scale. This is a large improvement compared to our old technique based on directly mixing oxides together, where a complex process of homogenization (iterative melting and milling) is needed. The measured emission spectrum is similar to commercial Yb doped fibers, except that the second broad emission wing is centered around 1020nm and not around 1060nm. However, the measured absorbance spectrum shows the same characteristics and matches the absorption spectra from commercial Yb doped fibers, which in turn enables the use of the standard ytterbium pump wavelengths (915nm & 976nm). The lifetime of the upper laser level of the ytterbium was determined to be τ=0.99ms. The single-clad fiber has a refractive index contrast between core and cladding of Δn=3.35 · 10^{-3} whereas the double-clad fiber features an index contrast of be Δn=2.65 · 10^{-3}, due so slightly different pure silica used for the particular claddings. The propagation losses of the single-clad LMA was measured to be 0.2dB/m at 633nm respectively 0.02414dB/m at 1550nm, which in turn shows that these fiber can be used for fiber laser respectively amplifier applications.

Right now we are in progress to measure the gain characteristic at 1030nm. In a next step, we will implement our sol-gel process using only optically passive elements such as e.g. germanium, titanium, graphene in order to realize passive fibers or fibers with a special functionality (graphene doped fiber). In addition we also want to implement other optically active rare earth elements (e.g. erbium) into our sol-gel process.

Our approach is also very well suited for the production of microstructured fibers such as leakage channel fibers (LCF), since we have the freedom regarding the geometry to realize any fiber structure and in addition we benefit from the fact that we can tailor the refractive index difference by controlling the (co-)dopant concentration. A first experiment already demonstrated the proof of principle for manufacturing such a LCF based on our sol-gel granulate material [21].

ACKNOWLEDGEMNT

This project was financially supported by the Swiss Commission for Technology and Innovation (CTI) under grant No. 17133.1. The authors thank Dr. W. Shin (Institute of since and technology, APRI, Gwangju – Korea) for vitrification experiments with the “small zone vitrification technique” and Christoph Bacher (Institute of applied physics, Bern - Switzerland) for his help and assistance during the fiber drawing.

REFERENCES

[1] Knight, J.C., et al., “Photonic crystal fibers,” Nature **424**, 847 (2003)
[2] Birks, T.A., et al., “Endlessly single-mode photonic crystal fibre,” Opt. Letters **22**, 961 (1997)
[3] Russell, P.St.J., et al., “Photonic-Crystal Fibers,” Journal of Lightwave Technology **24**, 4729 (2006)
[4] Poli, F., et al., “Photonic Crystal Fibers: Properties and Applications,” Springer Series in Materials Science **102**, (2007)
[5] Bjarklev, A., et al., [Photonic Crystal Fibres], Springer, (2003)

[6] Zervas, M., et al., “High power fiber lasers: A review," IEEE J. Sel. Top. Quantum Electron. **20**, 0904123 (2014).
[7] Seiki, O., et al., “Highly ytterbium-doped bismuth-oxide-based fiber,” Opt. Express **17**, 14104 (2009)
[8] Matesjec, V., et al., “Sol-Gel Fabrication and properties of silica cores of optical fibers doped with Yb^{3+}, Er^{3+}, Al_2O_3 or TiO_2,” Journal of Sol-Gel Science and Technology **13**, 617 (1999)
[9] Dong, L., et al., “All-Glass Large-Core Leakage Channel Fibers,” Journal of selected topics in quantum electronics **15** (1), (2009)
[10] Yeatman, E.M., et al., “Sol-Gel Fabrication of Rare-Earth Doped Photonic Components,” Journal of Sol-Gel Science and Technology **19**, 231 (2000)
[11] DiGiovanni, D.J., et al., “Structure and properties of silica containing aluminum and phosphorus near the AlPO4 join,” Journal of Non-Crystalline Solids **113**, 58 (1989)
[12] Tomozawa, M., et al.,”preparation of high purity silica glass,” J. non.Cryst. Solids **296,** 102-106 (2001)
[13] in collaboration with Dr. W. Shin from APRI (Advanced Photonics Research Institute, 123 Cheomdan-gwagiro (Oryong-dong), Buk-gu, Gwangju 500-712, Korea)
[14] Romano, V., et al., “Sol-gel based doped granulated silica for the rapid production of optical fibers,” International Journal of Modern Physics B **28**, 1442010 (2014)
[15] Etissa, D., et al., "Rare earth doped optical fiber fabrication by standard and sol-gel derived granulated oxides," Proc. SPIE 8426, (2012).
[16] Digonnet, M.J., [Rare-earth-doped fiber lasers and amplifiers], CRC Press, 2nd ed. (2001)
[17] Najafi, H., et al., “Atomic-scale imaging of dopant atoms and clusters in yb-doped optical fibers," Proc. SPIE 9886, paper 35 (2016).
[18] Raisin, P., et al., “High-precision confocal reflection measurement for two dimensional refractive index mapping of optical fibers,” Proc. SPIE 9507, (2015).
[19] el Sayed**,** A.**,** et al., “Two-dimensional refractive index profiling of optical fibers by modified refractive near-field technique,” Proc. SPIE 9744, (2016).
[20] el Sayed, A., et al., “High Spatial-Resolution Optical Time Domain Reflectometer for the Characterization of Doped Optical Fibers,” Master thesis, University of Bern, (2014)
[22] Scheuner, J., et al., “Design and realization of leakage channel fibres by the powder-in-tube method,” Proc. SPIE 9886, paper 39 (2016).